Pronounced Poly(methyl methacrylate) Dynamics Induced by Blending Morphology

F. M. Mulder,*,† B. J. P. Jansen,‡ P. J. Lemstra,‡ H. E. H. Meijer,‡ and H. J. M. de Groot†

Leiden Institute of Chemistry, Gorlaeus Laboratories, Leiden University, P. O. Box 9502, 2300 RA Leiden, The Netherlands, and Eindhoven University of Technology, P. O. Box 513, 5600 MB Eindhoven, The Netherlands

Received March 31, 1999

ABSTRACT: Abundant low-frequency motions in the poly(methyl methacrylate) (PMMA) phase of polymer blends of poly(propylene oxide) epoxy and thermoplastic PMMA with submicron morphologies are revealed by solid-state NMR measurements. The presence of this mobility is in line with the depression of glass temperatures in thin polymer films. The modified polymer dynamics induced by microscopic morphology is potentially important for research on frequency-dependent polymer conductivity, dynamics in polymeric glasses, physical aging, and models for polymer fracture dynamics.

Introduction

Large decreases of glass temperatures have been observed for polystyrene films with a thickness of 30−70 nm that were free-standing or supported on one side by a substrate.[1,2] Thin poly(methyl methacrylate) (PMMA) films were shown to have glass-transition temperatures that depended strongly on the bonding with the substrate on which they were placed.[3] A complete theoretical understanding of these effects is not available yet, but the decrease of the length scales of the morphology below correlation length scales of the bulk polymer will be a factor of key relevance. Such finite size effects may be expected to be also present in polymer blends with small, nanoscopic morphologies that are produced by a controlled phase separation. In this study microscopic dynamic properties of several PMMA/poly(propylene oxide) (PPO) blends at time scales that are typically of the order of 10^{-3}−10^{-6} s are assessed microscopically in a steady-state experiment using magic-angle spinning (MAS) solid-state NMR. We provide evidence that the steady-state low-frequency polymer mobility increases in large parts of the PMMA upon forming a morphology with submicron phase separation. Thus, PMMA, which is normally very rigid, is shown to become mobile by morphological confinement in these blends.

The mechanical properties of brittle glass-forming polymers, such as PMMA, can be improved considerably not only by the incorporation of rubbery domains[4] but also by tuning the morphology of the final blend.[5] The materials under investigation are more ductile and their toughness is improved by almost an order of magnitude[6,7] compared to bulk PMMA, which may be due in part to the observed high steady-state mobility in large fractions of the PMMA.

Materials and Methods

Blends consisting of PMMA (T_g = 395 K) and a rubbery epoxy resin (diglycidyl ether of poly(propylene oxide), SHELL Epikote 877) were cured using an aliphatic diamine (poly(propylene oxide) diamine, Hunstman Jeffamine D230). Since both the epoxy resin and the curing agent possess a poly(propylene oxide) backbone, the cured rubber phase (T_g = 240 K) is named PPO. The blends were prepared by polymerizing a homogeneous solution of methyl methacrylate (MMA), epoxy resin, curing agent, and three free-radical initiators. Upon increasing the temperature, two immiscible polymer networks are synthesized, which causes chemically induced phase separation. By carefully controlling the time−temperature profile, the morphology coarsening process after phase separation can be suppressed, and a morphology size in the range of tens of nanometers is obtained. This blending route was used to produce blends with PPO contents between 10 and 50 wt %. A detailed description of the materials synthesis and the morphology control is given in refs 6 and 7.

Crystalline or glassy polymer materials with little internal motion and which may be brittle show broad Gaussian-type ^{1}H NMR lines, up to 10^5 Hz wide, owing to the magnetic dipolar interaction between the nuclear spins. The homonuclear dipolar interactions in a rubber are motionally averaged, yielding narrow Lorentzian-type lines, down to 10^2 Hz wide. In an intermediate range of the polymer mobility, when there is a partial attenuation of the dipolar interactions, often a line shape is observed with an intermediate width and shape (related to a "stretched exponential" in the time domain).

Second, to probe the characteristic distance between mobile and less mobile parts, a ^{1}H T_2 filter is used, which selects magnetization from only the mobile protons, with narrow lines.[8,9] Subsequently, between two 90° pulses, this polarization can transfer between nuclei by ^{1}H spin diffusion that is mediated by the homonuclear dipolar couplings. The proton spectrum after spin diffusion can be measured directly, and from the line shape it is immediately obvious if mobile or rigid fractions are probed. The characteristic distance between the mobile and rigid phases can be determined from the initial slope of the plot where the narrow-line intensity is plotted against the square root of the spin-diffusion time.

Third, the 2D WISE heteronuclear correlation technique is applied to assign dynamics to the various polymer fractions.[10] A proton evolution time is followed by an adjustable longitudinal spin-diffusion period in which proton polarization can diffuse through the material. With subsequent cross-polarization, the proton encoded signals are transferred to specific carbon atoms, and high-resolution ^{13}C signals are detected. Appropriate phase cycling is applied to handle T_1 relaxation effects. The resulting 2D spectra show the proton line shape that can be detected in the different polymers. Subsequently

* Corresponding author. Present address: Interfaculty Reactor Institute, Delft University of Technology, Mekelweg 15, 2629 JB Delft, The Netherlands.
† Leiden University.
‡ Eindhoven University of Technology.

10.1021/ma9904619 CCC: $19.00 © 2000 American Chemical Society
Published on Web 01/05/2000

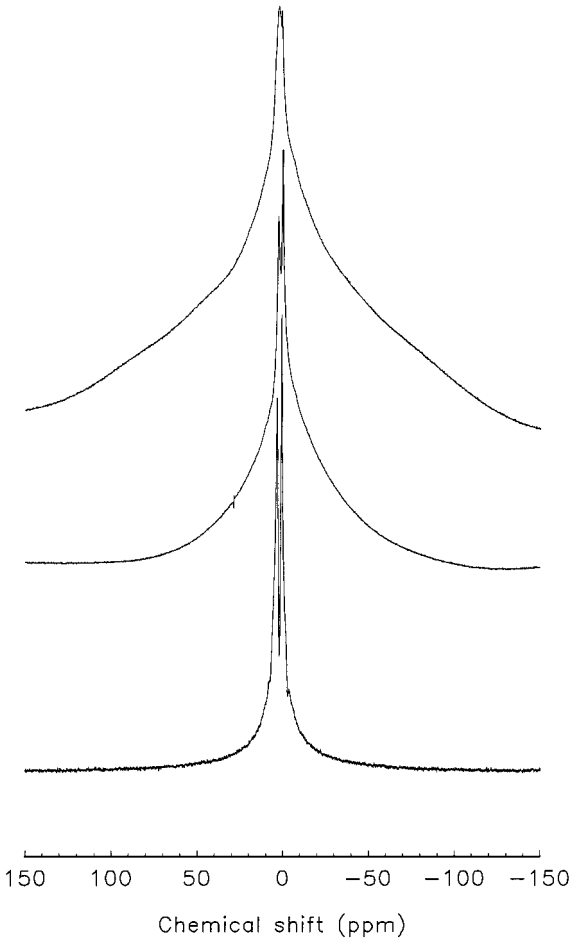

Figure 1. MAS proton spectra of blends of PMMA and PPO. Top to bottom: PMMA:PPO = 90:10, 80:20, 50:50. Data were collected using a modified 400 MHz MSL from Bruker with a spinning speed of 4.50 kHz. The radio-frequency field strength for the ^{1}H pulses corresponds with a nutation frequency of $\omega/(2\pi) = 50$ kHz.

this line shape can be used as a measure of the mobility of the specific polymers.

Fourth, by application of a ^{1}H T_2 filter followed by a relatively long cross-polarization period, the efficiency of the cross-polarization in the most mobile polymer fractions can be verified. All four NMR techniques are well-established, and they provide complementary and comprehensive information about dynamics, morphologies, and the spatial relation between these two phases on a microscopic scale.

Increased Low-Frequency Mobility in Blends of PMMA and a PPO Epoxy

All MAS NMR measurements were performed at room temperature (293 K). In Figure 1, the proton spectra of blends with different PPO contents are shown. A pronounced increase of the narrow fraction in the ^{1}H signals proves that the dynamics at time scales $\leq 10^{-4}$ s is enhanced by blending-induced phase separation with increasing amounts of PPO. There are six and eight protons per monomer in PPO and PMMA, respectively. The small ^{1}H chemical shift dispersion and overall similar signal properties prevent a straightforward assignment of the mobile fraction to PPO or PMMA. Much of the mobility observed is on a time scale of a few microseconds or less since it strongly reduces the proton dipolar couplings. A TEM picture of a 50% PMMA/PPO blend clearly shows the phase separation into PMMA (light) and PPO (dark) areas (Figure 2). The

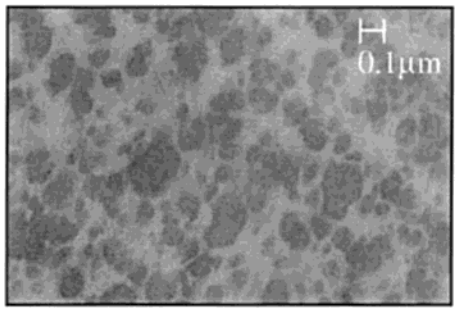

Figure 2. TEM picture of a stained PMMA/PPO = 50/50 blend. The dark and bright areas reveal phase separation on a scale of approximately 100 nm for this sample.

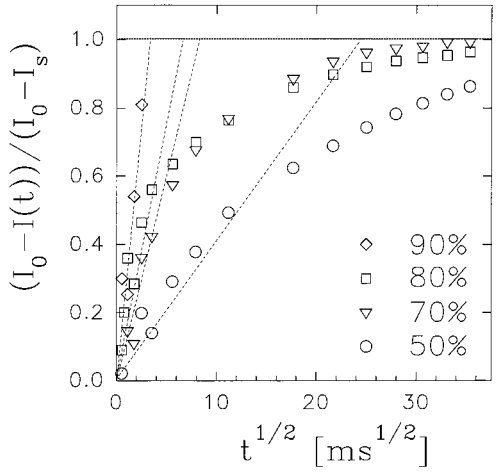

Figure 3. Results of the spin-diffusion measurement as described in the text. The intensity of the narrow fraction of the spectrum after spin diffusion, $[I(0) - \{I(t)\exp(t/T_1)\}]/(I(0) - I_s)$, is plotted versus the square root of the spin-diffusion period t. In this expression for $I(0)$ and I_s are the intensity at $t = 0$ and $t = \infty$, respectively. The exponential factor corrects for the loss of signal due to T_1 spin−lattice relaxation; T_1 is 0.8 s here. The dashed lines cross the saturation level at a time t_m^* that is used to calculate the characteristic domain size.[8,11]

typical PPO domain sizes appear to be about 90 ± 50 nm in diameter. The PMMA phase has thicknesses ranging roughly between 20 and 100 nm, where the thickness can be estimated from the PPO interdomain distance. These thicknesses are of the same order of magnitude as the film thickness that were used in ref 1. For the blends with less PPO, the PPO domains are too small for observation with TEM. However, for each compound, a typical length scale for distances between mobile and rigid polymer fractions was determined using the proton T_2 filtering and spin-diffusion methods described above.[8] In Figure 3 the spin-diffusion measurements are plotted. The domain sizes were extracted using the "initial rate approximation" for spin diffusion as described in refs 8 and 11. The effective spin-diffusion coefficient D_e is calculated from $D_e = 2(D_{PPO}D_{PMMA})^{1/2}/(D_{PMMA}{}^{1/2} + D_{PPO}{}^{1/2}) = 0.5$ nm^2 ms^{-1}, with the spin-diffusion coefficient in PMMA $D_{PMMA} = 0.8$ nm^2 ms^{-1} and in PPO $D_{PPO} = 0.1$ nm^2 ms^{-1}. The formula used for the domain size d is $d = (6/\pi^{1/2})[(D_e t_m^*)^{1/2}/(1 - f)]$, where f is the fraction of the total polarization that is selected by the T_2 filtering. The characteristic distances were estimated to be ≤10, ≈20, ≈30, and ≥120 nm in, respectively, the 10, 20, 30, and 50% PPO blends. The error margins are 25% since the spin-diffusion coefficient is only an effective one and the morphology will

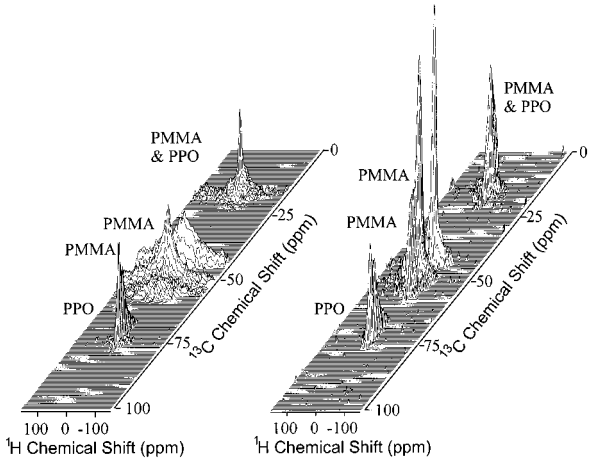

Figure 4. (a, left) ^{1}H−^{13}C WISE experiment on the 50:50 polymer blend. PMMA shows ^{13}C signals correlated with broad ^{1}H line shapes. A small narrow fraction on top of the broad shape around 50 ppm indicates mobile PMMA. The ^{13}C signals of PPO are correlated with narrow ^{1}H line shapes, indicating mobile PPO. The spinning speed was 4.50 kHz, and the cross-polarization had a duration of 250 μs. (b, right) ^{1}H−^{13}C WISE experiment with a proton spin-diffusion time of 50 ms revealing exchange of ^{1}H polarization between the most rigid parts and the more mobile parts of the 50:50 blend (spinning speed, 4.50 kHz; cross-polarization time, 250 μs). The ^{1}H line shape at the PPO positions does not change, while large changes are observed at the PMMA positions. This indicates that in this blend 50 ms is sufficient for polarization exchange between mobile and rigid parts of PMMA, while polarization exchange between the rigid PMMA and the mobile PPO is not yet observed. In this way it is observed that a fraction of 40% or more of the PMMA is mobile in this blend.

show a spread in domain sizes. For the blend containing 50% PPO, the mobile domain sizes determined from NMR are larger, albeit of the same order as the PPO domain sizes determined using TEM. This may suggest that a part of the PMMA is mobile in the material, in addition to the PPO. To summarize the results of the TEM and NMR morphology characterization for the 50% blend, it can be stated that PPO domain sizes will be smaller than, or equal to, the mobile domain size determined using the NMR procedures.

Heteronuclear WISE experiments including a variable spin-diffusion period were performed on the 50% PPO blend as displayed in Figure 4a,b. In Figure 4a the spin-diffusion period was suppressed by setting it to 0 ms, and a very short cross-polarization period of 250 μs was used. The ^{13}C responses of the PPO phase are correlated with narrow ^{1}H lines, and only a very little amount (<5%) of a broader signal. Thus at least 95% of the PPO polymer chains are mobile. Following the work of Landfester et al.,[12] this is an indication that there is negligible mixing of the PMMA and PPO. In their work on core−shell particles consisting of mobile poly(butyl acrylate) (PBuA) (T_g = −45 °C) and rigid PMMA, substantial immobilization of the PBuA was observed, which was attributed to a gradient in mixing at the molecular level. Here there is practically no such immobilization observed for the PPO phase. The ^{13}C signals from the PMMA phase are correlated with the broad proton lines that are characteristic for rigid polymers. The signal at 50 ppm has a relatively narrow component on top, indicative of more mobile PMMA. A very short cross-polarization period of 250 μs was used in order to ensure that the polarization transfer occurs over a short range only. The low cross-polarization

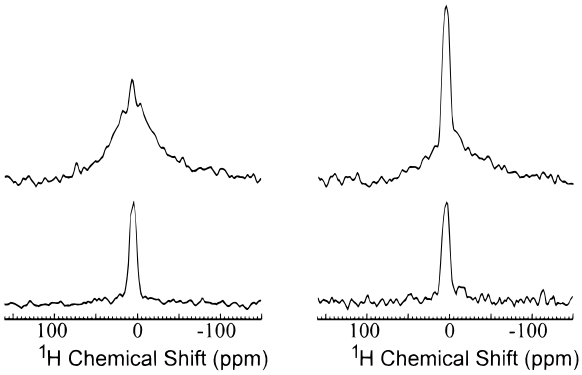

Figure 5. Top left and right plots: projections of the PMMA proton line shape at a ^{13}C chemical shift of 54 ppm in, respectively, parts a and b of Figure 4. Bottom left and right plots: projections of the PPO proton line shape at a ^{13}C chemical shift of 75 ppm in, respectively, parts a and b of Figure 4.

efficiency causes the mobile fractions of PPO and PMMA to be detected only weakly, but it has the advantage that one can be sure that only the nearest-neighbor protons are sampled and that a ^{13}C signal of PMMA only displays PMMA protons.

A WISE experiment with the spin-diffusion period set to 50 ms and the same short cross-polarization period of 250 μs was used to provide additional insight into the dynamics of the polymer chains (Figure 4b). The width and absolute intensity of the PPO response is the same as in Figure 4a. This shows that polarization transfer between the rigid PMMA phase and the mobile PPO phase must be very small for this spin-diffusion time limited to 50 ms. Polarization transfer between PMMA and PPO would have reduced the narrow PPO peak intensity, and simultaneously a broad feature of the rigid PMMA protons would have become evident at the PPO ^{13}C signals. This is obviously not the case. From Figure 3 we can find that there is polarization transfer from a mobile to a rigid phase in 50 ms, and the question arises as to where this can be observed in Figure 4b. For the responses of the PMMA, a major change of the line shape is detected after spin diffusion, since in Figure 4b the PMMA ^{13}C response is correlated with a strong narrow proton signal, while the intensity of the broad shape is strongly reduced. This may also be observed from Figure 5 where projections of a proton signal of PPO and of PMMA in the two WISE experiments are plotted. This result demonstrates that magnetization from mobile PMMA parts of the material has exchanged with polarization from the rigid PMMA parts, and this process can be efficiently detected by the cross-polarization in the rigid PMMA fraction. The total PMMA integrated signal following CP is about the same after 50 ms spin diffusion. This should be the case since it is determined by the rigid PMMA fraction in the material and by the overall homogeneous polarization in this experiment. From the intensities of the broad and narrow PMMA signals in Figure 4a,b, the fraction of mobile PMMA can be estimated to be at least 40%.

In the WISE experiment with zero spin-diffusion time in Figure 4a, the short cross-polarization time of 250 μs causes the mobile PMMA phases to be only weakly visible. Cross-polarization efficiencies are strongly dependent on the type of polymer and the time scale of the mobility that is present. It proved to be possible to observe the mobile PMMA directly after selection of the mobile fraction of the polymers using a ^{1}H T_2 filter, and

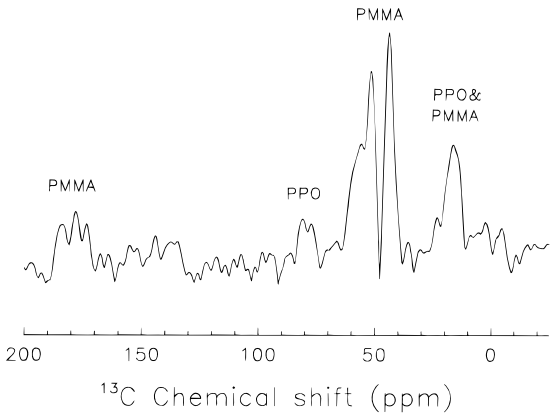

Figure 6. ^{1}H T_2 filtered ^{13}C CPMAS spectrum showing mobile fractions of the 20:80 polymer blend. The ^{1}H T_2 filtering time of 100 μs is sufficient to suppress the signal from rigid bulk PMMA effectively. With a cross-polarization time of 2 ms, the mobile PMMA fraction can be detected in the ^{13}C domain. The spectral contributions of PPO and PMMA are still quite weak owing to the low cross-polarization efficiencies of these mobile polymers. The spinning speed was 4.50 kHz.

using a significantly longer cross-polarization period of 2 ms (Figure 6). A control experiment on pure bulk PMMA with the same experimental conditions gave a negligible PMMA signal.

The pronounced mobility of PMMA in large parts of the blend cannot be attributed to remnant mixing of PMMA and PPO since the mobile fraction of material is located much closer to the rigid fraction of PMMA than to the PPO: after spin diffusion in the WISE experiments, strong narrow signals appear at the PMMA line positions, and not at the PPO line position. A small amount of less than ±5% of PPO mixed in the PMMA phase cannot be excluded, but this cannot explain the large effects that are observed experimentally. This may also be concluded from the 10% PPO blend, which has only little phase separation and shows a proton spectrum consistent with mostly rigid polymers in the material.

The mobility in both PPO and fractions of the PMMA in principle may allow the phase-separation process to continue in those microscopic areas where PMMA is mobile. The final morphology formed has to be arrested by cross-linking PPO as was done here. The important finding is the large effect of softening of the PMMA mobility modes in a significant fraction of the PMMA phase. This mobility results from the microscopic morphology.

Conclusions

Experimental evidence that the dynamics of PMMA can be strongly modified by its confinement to a certain morphology is provided using MAS NMR techniques on blends of phase-separated PMMA and PPO. A submicron morphology of polymer blends provides a means to tune the microscopic mobility of polymers at time scales of milliseconds to microseconds.

Acknowledgment. This work is part of the research program of the "Stichting Technische Wetenschappen (STW)", which was financially supported by the "Nederlandse Organisatie voor Wetenschappelijk Onderzoek" (NWO).

References and Notes

(1) Forrest, J. A.; Dalnoki-Veress, K.; Stevens, J. R.; Dutcher, J. R. *Phys. Rev. Lett.* **1996**, *77*, 2002.
(2) Jean, Y. C.; Zhang, R.; Cao, H.; Yuan, J. P.; Huang, C. M.; Nielsen, B.; Asoka-Kumar P. *Phys Rev. B* **1997**, *56*, R8459.
(3) Keddy, J. L.; Jones, R. A. L.; Cory, R. A. *Europhys. Lett.* **1994**, *27*, 59.
(4) See, for example: Wu, S. *Polym. Eng. Sci.* **1990**, *30*, 753.
(5) van der Sanden, M. C. M.; Meijer, H. E. H.; Lemstra, P. J. *Polymer* **1993**, *34*, 2148.
(6) Jansen, B. J. P.; Meijer, H. E. H.; Lemstra, P. J. *Polymer* **1999**, *40*, 2917.
(7) Jansen, B. J. P.; Tamminga, K. Y.; Lemstra, P. J. *Polymer* **1999**, *40*, 5601.
(8) Schmidt-Rohr, K.; Spiess, H. W. *Multidimensional Solid-State NMR and Polymers*; Academic Press: London, 1994.
(9) Blümich, B. *Concepts Magn. Reson.* **1998**, *10*, 19−31.
(10) Schmidt-Rohr, K.; Clauss, J.; Spiess, H. W. *Macromolecules* **1992**, *25*, 3273.
(11) Claus, J.; Schmidt-Rohr, K.; Spiess, H. W. *Acta Polym.* **1993**, *44*, 1.
(12) Landfester K.; Boeffel, C.; Lambla, M.; Spiess, H. W. *Macromolecules* **1996**, *29*, 5972−5980.

MA9904619